THYROID
Volume 22, Number 9, 2012

DOI: 10.1089/thy.2010.0400

Hypothyroidism in the Adult Rat Causes Incremental Changes in Brain-Derived Neurotrophic Factor, Neuronal and Astrocyte Apoptosis, Gliosis, and Deterioration of Postsynaptic Density

Claudia Cortés,[1] Eliseo Eugenin,[2] Esteban Aliaga,[3] Leandro J. Carreño,[4] Susan M. Bueno,[4] Pablo A. Gonzalez,[4] Silvina Gayol,[5] David Naranjo,[5] Verónica Noches,[1] Michelle P. Marassi,[6] Doris Rosenthal,[6] Cindy Jadue,[1] Paula Ibarra,[1] Cecilia Keitel,[7] Nelson Wohllk,[7,8] Felipe Court,[9] Alexis M. Kalergis,[4,10] and Claudia A. Riedel[1]

Background: Adult hypothyroidism is a highly prevalent condition that impairs processes, such as learning and memory. Even though tetra-iodothyronine (T_4) treatment can overcome the hypothyroidism in the majority of cases, it cannot fully recover the patient's learning capacity and memory. In this work, we analyzed the cellular and molecular changes in the adult brain occurring with the development of experimental hypothyroidism.
Methods: Adult male Sprague-Dawley rats were treated with 6-propyl-2-thiouracil (PTU) for 20 days to induce hypothyroidism. Neuronal and astrocyte apoptosis were analyzed in the hippocampus of control and hypothyroid adult rats by confocal microscopy. The content of brain-derived neurotrophic factor (BDNF) was analyzed using enzyme-linked immunosorbent assay (ELISA) and *in situ* hybridization. The glutamatergic synapse and the postsynaptic density (PSD) were analyzed by electron microscopy. The content of PSD proteins like tyrosine receptor kinase B (TrkB), p75, and N-methyl-D-aspartate receptor (NMDAr) were analyzed by immunoblot.
Results: We observed that the hippocampus of hypothyroid adult rats displayed increased apoptosis levels in neurons and astrocyte and reactive gliosis compared with controls. Moreover, we found that the amount of BDNF mRNA was higher in the hippocampus of hypothyroid rats and the content of TrkB, the receptor for BDNF, was reduced at the PSD of the CA3 region of hypothyroid rats, compared with controls. We also observed that the glutamatergic synapses from the stratum radiatum of CA3 from hypothyroid rats, contained thinner PSDs than control rats. This observation was in agreement with a reduced content of NMDAr subunits at the PSD in hypothyroid animals.
Conclusions: Our data suggest that adult hypothyroidism affects the hippocampus by a mechanism that alters the composition of PSD, reduces neuronal and astrocyte survival, and alters the content of the signaling neurotrophic factors, such as BDNF.

Introduction

Thyroid hormones tri-iodothyronine (T_3) and tetra-iodothyronine (T_4) are essential for appropriate brain development and function (1–5). Hypothyroidism is highly prevalent worldwide and is characterized by low plasma levels of T_4 and high plasma levels of thyroid stimulating hormone (TSH). Hypothyroidism in the adult reduces cell metabolism in almost all tissues of the body (6). At the brain level, adult hypothyroid patients show cognitive

[1]Millennium Institute on Immunology and Immunotherapy, Department of Biological Sciences, Faculty of Biological Sciences and Faculty of Medicine, Andrés Bello University, Santiago, Chile.
[2]Department of Pathology, Albert Einstein College of Medicine, Bronx, New York.
[3]Neurobiology and Plasticity Development Center, Department of Physiology; [5]Interdisciplinary Center of Neurosciences; University of Valparaíso, Valparaíso, Chile.
[4]Millennium Institute on Immunology and Immunotherapy, Department of Molecular Genetics and Microbiology, Faculty of Biological Sciences; [9]Millennium Nucleus for Regenerative Biology, Faculty of Biological Sciences; [10]Department of Rheumatology, Faculty of Medicine; Pontifical Catholic Universty of Chile, Santiago, Chile.
[6]Carlos Chagas Filho Institute of Biophysics, University of Rio de Janeiro, Rio de Janeiro, Brazil.
[7]Institute of Advanced Medical Studies, Santiago, Chile.
[8]Salvador Hospital, University of Chile, Santiago, Chile.

deterioration, memory impairment, and depression symptoms (7,8). Regretfully, patients that have been properly treated with T_4 to overcome their hypothyroid condition have not always fully recovered from the symptoms affecting the central nervous system (CNS), such as the memory capacity (9–11). These alterations have also been observed in animal models as adult rats, in which hypothyroidism is associated with deterioration of their memory and learning capacity (12) and impairment of long-term potentiation (13). In adult rats hypothyroidism causes, at the molecular level, altered expression of mRNA encoding for the subunits comprising the N-methyl-D-aspartic receptor (NMDAr) (14), and the tyrosine kinase receptor (TrkB) (15). A reduction in the number of neurons in the hippocampus has also been reported in the adult hypothyroid rats (16). Given the high frequency of hypothyroidism in the human population, it is essential to understand the cellular and molecular mechanisms that are altered by this disorder. In this study, we have analyzed the cellular and molecular effects of adult hypothyroidism in the telencephalon and, particularly, in the hippocampus and parietal cortex. We observed by a quantitative analysis that adult hypothyroidism leads to a reduction in thickness of the postsynaptic densities (PSDs). Further, PSDs from hypothyroid telencephalon showed reduced expression of important molecules, such as the N-methyl-D-aspartate receptor 1 (NR1), N-methyl-D-aspartate receptor 2 A/B (NR2A/B), and TrkB. In contrast, the brain-derived neurotrophic factor (BDNF) peptide levels were fivefold higher in hypothyroid telencephalon, compared with control animals. Specifically, the hippocampus of hypothyroid rats displayed higher content of BDNF mRNA. In addition, all these changes were associated with gliosis and neuronal death at the hippocampus. These observations support the notion that hypothyroidism is harmful for the hippocampus and neocortex.

Materials and Methods

Induction of hypothyroidism in adult rats

Male Sprague-Dawley rats, weighing 250–280 g, were treated with 0.05% of 6-propyl-2-thiouracil (PTU; Sigma) in drinking water for 20 days to induce hypothyroidism, as described previously (17). A control group of rats received drinking water without PTU. Serum samples from both PTU-treated and normal rats were obtained to analyze levels of thyroid hormones T_3, T_4, and TSH. Serum levels of total T_3 (tT_3) and free T_4 (fT_4) were measured by chemioluminescence in the laboratory of Institute of Advanced Medical Studies (IEMA), Santiago, Chile (18). Radioimmunoassay was used to measure TSH at the Carlos Chagas Filho Institute of Biophysics of Federal University of Rio de Janeiro, Brazil. The levels of thyroid hormones found in our rat serum were similar to those previously reported in the literature (19). All animal work was performed according to the Guide for Care and Use of Laboratory Animals (National Institute of Health), the approval of the Andrés Bello University Bioethics Committee, and the institutional guidelines were overseen by a veterinarian.

Immunofluorescence and apoptosis assays

Coronal brain sections of 30 μm thickness were cut between 2.16 and 4.56 mm from Bregma by cryostate. These sections were fixed and permeabilized in 70% ethanol and then incubated in terminal deoxynucleotidyl transferase dUTP nick end labeling (TUNEL) reaction mixture at 37°C for one hour (Roche). The tissue sections were washed and incubated in blocking solution at room temperature. These tissue sections were then incubated overnight with the primary antibody mix: monoclonal anti–glial fibrillary acidic protein (GFAP) (1:1000; Sigma) and polyclonal anti–microtubule-associated protein (MAP)-2 (1:300; Sigma). Fixed sections were washed, incubated with Cy3-conjugated anti-rabbit immunoglobulin G (IgG) (Sigma; 1:300) and Cy5-conjugated anti-mouse antibody (1:300; Invitrogen) for one hour at room temperature, followed by a one hour phosphate-buffered saline (PBS) wash. Tissue sections were mounted using Prolong Gold® (Molecular Probes) and examined by confocal microscopy (Leica AOBS). To identify the apoptotic neurons or astrocytes, a double immunofluorescence staining for each cell type was performed as described (TUNEL and anti-MAP-2 and TUNEL and anti-GFAP respectively) (20,21). Specificity was confirmed by replacing the primary antibody with the appropriate isotype-matched control reagent, anti-IgG2A, or the IgG fraction of normal rabbit serum (Santa Cruz Biotechnology). Quantification of neuronal and astrocyte apoptosis was performed by counting the total number of nucleus and the number of TUNEL positive nucleus in GFAP and MAP-2 positive cells in the field. For each condition, four rat brains were analyzed and three slices were studied for each brain. Data were expressed as the percentage of apoptotic neurons or astrocytes in the field respectively.

In situ hybridization detection of BDNF mRNA

Brain tissue was fixed by transcardiac perfusion of 3% paraformaldehyde in 0.1 M PBS pH 7.4. After fixation, brains were removed and postfixed at 4°C during 2 hours in the same fixative and then cryoprotected in 25% sucrose solution in 0.1 M PBS at least during 48 hours at 4°C. *In situ* hybridization studies using a non-isotopic riboprobe were performed as previously described (22), but modified for mounted sections. Briefly, 16 μm thick-sections from experimental and control rats were cut on a Leica cryostat and selected sections from the hippocampus and parietal cortex regions were mounted on poly-L-lysine-coated glass slides. Sections were brought to room temperature, rinsed three times in PBS (10 minutes each), and then prehybridized during 2 hours at 50°C in hybridization buffer (60 mM Tris-HCl [pH 7.4], 50% formamide, 0.6 M NaCl, 0.4 mM ethylenediaminetetraacetic acid [EDTA, pH 8.0], 1× Denhardt's solution, 400 μg/mL denatured salmon testis DNA, and 2 mg/mL sarcosyl). Then, for each slide containing five brain sections, a saturating amount of digoxigenin-11-UTP-labeled riboprobe (100 ng/mL) was added to the hybridization buffer. The cRNA antisense probe was specific for the coding exon (exon V) of BDNF and has been previously used in rat brain tissue (23). To allow hybridization, coverslips were placed over the sections, which in turn were placed in humidified glass chambers overnight at 50°C. Then, post-hybridization treatment and incubation with alkaline phosphatase-conjugated anti-digoxigenin antibody (Roche) were performed as described (24). Finally, alkaline phosphatase reaction was visualized by incubation with 4-nitro blue tetrazolium and 5-bromo-4-chloro-3-indolyl-phosphate (Roche). Controls were

carried out on the sections with a sense riboprobe. *In situ* hybridization signals were analyzed on a PC computer using the public Scion Image software analysis program (Scion Corp: www.scioncorp.com). In the *in situ* hybridization experiments label intensity was calculated as the mean value of optical density (sampled cell by cell using the function "Quantify" and "Mean Intensity" after selecting the whole somatic region). Measurements were performed on 20–25 cells from each cerebral region or cortical layer, from a total of three independent experiments and expressed as a percentage of the control.

BDNF quantification

The content of BDNF was analyzed in 7 mg of the total telencephalon homogenate. The homogenate was centrifuged at 20,000 *g* in a MIKRO 22R Hettich Centrifuge at 4°C for 30 minutes. The supernatant was discarded and the pellet was resuspended in a solution containing 137 mM NaCl, 20 mM Tris-HCl (pH 8.0), 1% nonidet P-40 (NP40), 10% glycerol, 1 mM of phenylmethylsulfonyl fluoride, 10 μg/mL aprotinine, 1 μg/mL leupeptine, and 0.5 mM sodium vanadate. The samples were sonicated with three pulses for 15 seconds at intensity 4, with 5-s intervals in a Misonix Sonicator Ultrasonic processor XL. After sonication, samples were centrifuged at 16,000 *g* for 30 minutes at 4°C in a MIKRO 22R Hettich Centrifuge. Aliquots of 100 μL of the supernatants were mixed with 40 μL of a solution containing 137 mM NaCl, 2.68 mM KCl, 1.47 mM KH_2PO_4, 8.1 mM Na_2HPO_4 (pH 7.35), 0.9 mM $CaCl_2$, and 0.5 mM $MgCl_2$. Then, 20 μL of HCl 1 M was added, incubated for 15 minutes and neutralized with 20 μL of 1 N of NaOH. The samples were kept at −80°C until use. The content of BDNF in these extracts was analyzed by BDNF Emax® Immunoassay System (Promega) as described previously (25). Briefly, a 96-well plate was coated with anti-BDNF monoclonal antibody (20 ng/well) and incubated at 4°C overnight. Then, the plate was washed with a buffer containing 150 mM NaCl, 0.05% Tween 20, and 20 mM Tris-HCl (pH 7.6) and blocked with 200 μL of 1× blocking solution, for one hour. Plates were then washed with 150 mM NaCl, 20 mM Tris-HCl, and Tween® 20 0.05% buffer (TBST), and 100 μL of sample was added in triplicate to each well and incubated for 2 hours at 4°C. Then, the plate was washed five times using TBST buffer and 100 μL of anti-human BDNF polyclonal antibody (diluted to 1:500) was added to each well and incubated for 2 hours. The plate was again washed with TBST buffer and incubated with 100 μL of 1:200 dilution of anti-IgG horseradish peroxidase (HRP) conjugate for one hour at room temperature. The plate was washed five times with TBST buffer and antibody binding was evidenced by adding 100 μL Promega 3,3′,5,5′-tetramethylbenzidine solution until color development was evident. This reaction was stopped with 100 μL of 1 N HCl. The absorbance was measured at 450 nm in a plate reader (Nunc-Immuno™). The BDNF concentration was calculated using a BDNF standard and expressed as picogram of BDNF/mg of protein.

TrkB immunohistochemistry

Rats were perfused via the left ventricle using peristaltic pump (WP, Peri-Star), first with PBS, then with a solution containing 4% of paraformaldehyde (Merck), 0.3% of picric acid (Sigma), and 0.1% of glutaraldehyde (Sigma) in PBS pH 7.4. Brains were removed and incubated in the same fixation solution with 10% sucrose (Sigma), and then 30% sucrose solution. Floating coronal brains slices of 30 μm thick were obtained using a cryostat (Leica, CM 1510). Floating sections were incubated with 0.5% hydrogen peroxidase, then with the blocking solution (3% of normal goat serum [Sigma] in PBS, pH 7.4). The floating sections were first incubated with 0.05 μg/mL of polyclonal anti-TrkB (SC-12, Santa Cruz Biotechnology, Inc.), then with 1.5 μg/mL of biotinylated goat anti-rabbit (BA-1000, Vector Laboratories), and with avidin-biotin peroxidase enzyme conjugated (ABC Kit, Vector Laboratories) at a dilution 1:250. The specific binding of the anti-TrkB antibody was revealed after incubating the floating sections with 0.05% (w/v) 3,3′-diaminobenzidine, 0.01% H_2O_2, and 0.25% nickel chloride in PBS. The tissues sections were analyzed in a Leica DM 2000 microscope. Three brain slices were analyzed per rat and three rats were used in this study.

Isolation of PSDs

PTU-treated and control male rats were decapitated with a guillotine and their brains were isolated. The telencephalon was dissected, cut, and homogenized on ice in 8 mL of homogenization buffer (0.32 M sucrose, 0.5 mM EDTA, and 5 mM Tris pH 7.4), using 12 strokes with a 40 mL Tissue Grind Potter with Teflon Pestle (Thomas Scientific). One milliliter of each brain homogenate was saved to analyze the total amount of protein. Then, the telencephalon homogenate was centrifuged at 1000 *g* for 10 minutes at 4°C, using a Sorvall centrifuge 5B-plus with a SS-34 rotor. The supernatant (s1) was saved and the pellet (P1) was washed with homogenization buffer and manually homogenized on ice using Tissue Grind Potter. Then, this fraction was centrifuged at 1000 *g* for 10 minutes at 4°C. The second pellet obtained (P2) was discarded and the supernatant (s2) was mixed with s1. s1 + s2 were centrifuged at 12,000 *g* in a Sorvall 5B-plus, with a SS-34 rotor, for 20 minutes at 4°C. The third pellet (P3) was saved and rinsed with solution A (0.32 M sucrose, 5 mM Tris-HCl pH 8.1, 0.5 mMethylene glycol tetraacetic acid, and 1 mM dithiotreitol) and manually homogenized with a 17 mL Tissue Grind Potter with Teflon Pestle (Thomas Scientific). The homogenized P3 was loaded on a discontinuous sucrose step gradient (0.32, 1, 1.2 M sucrose in 5 mM Tris-HCl pH 8.1) and centrifuged at 150,000 *g* for 2 hours at 4°C, using a AH629 Sorvall rotor. The synaptosome 1 fraction (Syn1) was isolated from 1 to 1.2 M fraction of the sucrose gradient, diluted 10 times with lysis buffer (5 mM Tris-HCl pH 8.1 and 0.5 ethylene glycol tetraacetic acid) and lysed by gently mixing with magnetic agitation on ice for 30 minutes. Then the lysed Syn1 fraction was centrifuged at 33,000 *g* for 30 minutes in a Sorvall 5B plus rotor SS34. The pellet obtained after this centrifugation step (P4) was resuspended in 3 mL of solution A and manually homogenized. Then P4 was loaded on a discontinuous sucrose step gradient (0.32, 1, and 1.2 M sucrose in 5 mM Tris-HCl pH 8.1) and centrifuged at 250,000 *g* for 2 hours at 4°C, using the AH629 Sorvall. The fraction of synaptosomes 2 (S2) was obtained from 1 to 1.2 M fractions. S2 was saved and diluted with eight volumes of 0.32 M sucrose, 0.025 mM $CaCl_2$, 1% Triton X-100, 2 mM dithiothreitol, and 10 mM Tris-HCl pH 8.1. Then, the S2 was gently mixed in this buffer and centrifuged at 33,000 *g* (Sorvall RC5B plus rotor SS34) for 30

minutes at 4°C. The fifth pellet (P5) is the PSD fraction. This fraction was washed with 50 mM HEPES pH 7.4 and centrifuged at 250,000 *g* (Beckman Optima TLX, rotor TLA110) for 10 minutes at 4°C. The sixth pellet was resuspended in 50 mM HEPES pH 7.4, frozen in liquid nitrogen, and stored at −80°C until use.

Immunoblot for postsynaptic proteins

Protein concentration in the PSD fraction, and total telencephalon homogenate samples were determined by the bicinchoninic acid method, as described previously (26). The PSD and total homogenate samples were diluted 1:1 with loading buffer and heated at 100°C for 5 minutes. Then, 20 and 40 μg of protein, respectively, were loaded on a 10% sodium dodecyl sulfate-polyacrylamide gel electrophoresis (SDS-PAGE), resolved by electrophoresis, and electrotransferred to a nitrocellulose membrane (Thermo Scientific). The nitrocellulose membranes were incubated one at a time with (i) 1/1000 dilution of anti-NR1 antibody (Chemicon, catalog no. AB1516) for 1 hour; (ii) 1/1000 dilution of anti-NR2A/B antibody (Chemicon, catalog no. AB1548W) for 1.5 hours at room temperature; (iii) 1/1000 dilution of anti-P75 antibody (Upstate, catalog no. 07-476) for 1 hour at room temperature; (iv) 1/1000 dilution of anti-PSD-95 antibody (Chemicon, catalog no. MAB377) for 16 hours at 4°C; (v) 1/1000 dilution of anti-TrkB antibody (Transduction, catalog no. 610102) for 16 hours at 4°C; and (vi) 1/1000 dilution of anti-β-tubulin antibody (Sigma, catalog no. T8660) for 16 hours at 4°C. A HRP-conjugated goat anti-rabbit IgG (Calbiochem, catalog no. 401215) or HRP-conjugated goat anti-mouse IgG (Calbiochem, catalog no. 401315) was used as secondary antibody. Both of these secondary antibodies were diluted to 1/1500 and incubated with the nitrocellulose for one hour at room temperature. The immunoblots were revealed using the enhanced chemioluminescence Western blot detection system (ECL, Amersham).

Immunoprecipitation

The NR2A subunit of the NMDA receptor was immunoprecipitated from synaptosome 2 fraction (S2) obtained from PTU-treated and control rats, to analyze the composition of NMDA receptor in this fraction. The S2 isolated was denatured and solubilized as previously described (27). Briefly, S2 was centrifuged at 100,000 *g* for 30 minutes at 4°C (Beckman TLX, rotor TLA110). The pellet was resuspended and solubilized at 37°C for one hour in radioimmunoprecipitation assay buffer containing 50 mM Tris pH 9.0, 150 mM NaCl, 1% bovine serum albumin, 1 mM EDTA, 1% NP40, 1% sodium deoxycholate, 0.1% SDS, 1 mM phenylmethylsulfonyl fluoride, 3.3 μg/mL leupeptin, 0.1 mM sodium fluoride, 0.5 mM sodium o-vanadate, and 0.5 mg/mL aprotinin. Then samples were centrifuged at 100,000 *g* for 60 minutes at 4°C (Beckman TLX, rotor TLA110). The supernatant of S2 (detergent soluble portion of synaptic membranes) was dialyzed overnight at 4°C in 0.32 M sucrose, 0.05 mM Tris pH 7.5, 10 μM EDTA, 0.1% Triton X-100. In parallel, 5 μg of an antibody against the NR2A subunit (Zymed, catalog no. 32-0600) was preincubated with 50 μL of protein G-sepharose beads (GE Healthcare, catalog no. 17-0618-01) in 0.5 mL of 0.05 M Tris-HCl pH 7.5; 10 μM EDTA; and 0.1% Triton X-100. The dialyzed samples were centrifuged at 100,000 *g* for one hour at 4°C (Beckman TLX, rotor TLA110). The supernatants were incubated with protein G-sepharose beads for 60 minutes at 4°C with agitation. After this treatment, the supernatants were centrifuged at 6000 *g* for 5 minutes, and half of the supernatant volume was added to protein G-sepharose-antibody complex (General Electric) and incubated for 5 hours at 4°C with agitation. The beads were washed twice in buffer that contained 0.05 M Tris-HCl pH 7.5, 10 μM EDTA, and 0.1% Triton X-100, and twice with the same buffer plus 0.5 M LiCl. The beads and samples of supernatant were boiled for 5 minutes in loading buffer (two-fold concentration). Finally, the samples were analyzed by Western blotting. The content of each protein was quantified by a densitometric analysis of each detection band. Then these values were corrected by the loading factor. The loading factor was obtained from the densitometric analysis of the tubulin band.

Transmission electron microscopy

Rats were perfused via left ventricle with 0.1 M PBS pH 7.4 followed with 2% of glutaraldehyde and 4% of paraformaldehyde in PBS. The hippocampi were dissected from the telencephalum and incubated by immersion with the same fixative solution. Tissue blocks were postfixed in 3% glutaraldehyde in 0.1 M sodium cacodylate buffer pH 7.2 for 6 hours, followed by fixation in 1% of osmium tetroxide. Then the hippocampi were stained with 2% of uranyl acetate aqueous followed by dehydration with ascendant acetone solution and subsequently were pre-embedded in epon: acetone 1:1 and then with pure epon. Semithin sections of 1 μm were stained with 1% toluidine blue. Thin sections of 80 nm hippocampi were stained with 4% of acetate.

PSDs were purified as described in the PSD isolation protocol. The PSD pellets were collected and fixed in PBS with 2.5% of glutaraldehyde. Then, the PSD were centrifuged at 250,000 *g* for 12 minutes (Beckman TLX, TLA110 rotor). The pellet was postfixed with 1% osmium tetroxide. After this the samples were stained with 2% of uranyl acetate aqueous. PSD were dehydrated in ascendant alcohol and embedded in EPON812 resin. PSD sections between 0.6 and 0.7 nm thicknesses were cut using ultramicrotome (Sorvall, model MT2). The CA3 hippocampi and the PSDs fractions were observed and microphotographed with Zeiss EM-109 transmission electron microscope Philips Tecnai 12 Bio Twin at 80 kV at the Unidad de Microscopía Electrónica of the Pontificia Universidad Católica de Chile.

Statistical analyses

Unpaired two-tailed *t*-tests were performed on the experimental data shown here. The Sigma Plot9 plus sigma Stat 3.5 program Systat Software, Inc. was used for the analyses. The results were considered to be significantly different when $p < 0.05$.

Results

Hypothyroidism induction in adult rats

After 20 days of PTU treatment, serum samples were collected from PTU-treated and control rats to analyze the serum levels of tT_3, fT_4, and TSH (Fig. 1). PTU-treated rats

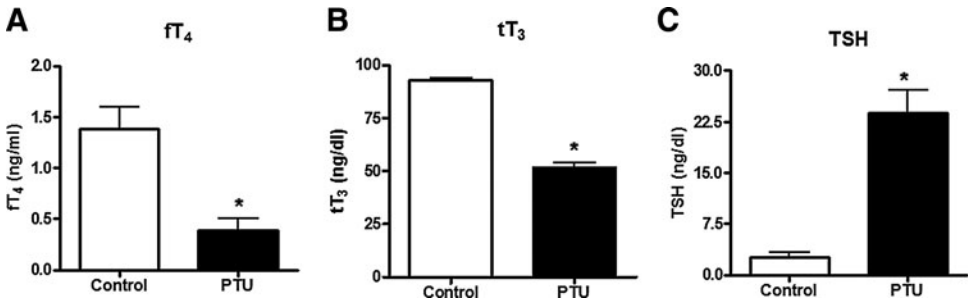

FIG. 1. PTU treatment induces hypothyroidism in adult rats. Serum levels of fT_4, tT_3, and TSH were determined in adult rats non-treated (control) or treated with PTU for 20 days (see "Materials and Methods"). **(A)** Mean values for fT_4 levels (ng/mL) ± SEM of PTU ($n=3$) and control rats ($n=3$). **(B)** Mean values for tT_3 levels (ng/dL) ± SEM of PTU ($n=3$) and control rats ($n=3$). **(C)** Mean values for TSH levels (ng/dL) ± SEM of PTU ($n=3$) and control rats ($n=3$). Significant differences (*) were observed at the levels of fT_4, tT_3, and TSH among control and PTU-treated rats ($p<0.05$). PTU, 6-propyl-2-thiouracil; tT_3, total tri-iodothyronine; fT_4, free tetra-iodothyronine; TSH, thyroid stimulating hormone; SEM, standard error of the mean.

showed significantly reduced serum levels of fT_4 (control: 1.4 ± 0.4 ng/mL; PTU-treated rats: 0.4 ± 0.2 ng/mL, $n=3$, $p<0.05$; Fig. 1A), tT_3 (control: 92.9 ± 1.9 ng/dL; PTU-treated rats: 51.8 ± 3.9 ng/dL, $n=3$, $p<0.05$; Fig. 1B) and significantly increased TSH serum levels (control: 2.5 ± 1.3 ng/dL and PTU-treated rats: 23.8 ± 5.9 ng/dL, $n=3$, $p<0.05$) compared with normal rats (Fig. 1C). Based on the clinical definition of hypothyroidism, the serum levels of tT_3, fT_4, and TSH indicated that the PTU treatment induced a hypothyroid condition in these animals.

Hypothyroidism promotes apoptosis and gliosis in the adult rat brain

To evaluate whether induction of hypothyroidism in adult rats alters the survival of neurons and astrocytes in the hippocampus, tissue sections were obtained from control and hypothyroid animals and stained for the following marker: TUNEL to determine apoptosis, the neuronal marker MAP-2, the glial marker GFAP to determine gliosis, and a nuclear staining (DAPI). Then, quantification of these parameters was performed by confocal microscopy. As shown in Figure 2A and B, a low level of neuronal and astrocyte apoptosis was observed in the hippocampus of normal adult rats, however, the hippocampus obtained from hypothyroid adult rats showed a significant increased level of apoptosis in neurons and astrocytes. Moreover, we observed that astrocyte apoptosis was higher than neuronal apoptosis and that both were significantly different in hypothyroid rats compared with control rats (Fig. 2B). Negative controls with non-immune sera, IgG1 control or no enzyme for TUNEL staining were included in all experiments (Fig. 2A).

Further, using quantification of positive pixel for each channel, we also observed a reduction in MAP-2 staining in the hippocampus of hypothyroid rats, compared with normal animals (Fig. 2C, neurons). Because the reduction of MAP-2 was higher than the total number of neuronal apoptosis, we suggest that MAP-2 reduction is not only due to neuronal cell death, but also due to changes in length, diameter, and number of neuronal processes. In contrast to the reduction of MAP-2, we observed an increased staining for GFAP in the hippocampus of hypothyroid rats, compared with normal animals (Fig. 2C, astrocytes), suggesting that gliosis occurs in hypothyroid animals.

Hypothyroid adult brains show altered contents of BDNF and TrkB

It has been reported that BDNF could play opposite effects in neuronal survival and synapsis potentiation depending in part on which type of receptor is expressed in the target cell (28). TrkB and p75 are the specific and non specific receptors for BDNF, respectively (28). Therefore, we measured both the mRNA and protein expression level of BDNF and its receptors TrkB and p75 in the brain of PTU-treated and control rats. The BDNF mRNA level was studied by an *in situ* hybridization assay, using the exon V as the hybridization target, which is the common exon among the four different forms of BDNF mRNAs. The hybridization signals for BDNF exon V mRNA showed a significant increase in layers II, III, and V of the parietal cortex, dentate gyrus, CA1, and CA3 hippocampal regions of PTU-treated animals, compared with the expression levels shown by control animals (Fig. 3A, B). In agreement with this result, we determined by enzyme linked immunosorbent assay (ELISA) that BDNF peptide level was increased fivefold in telencephalon derived from PTU-treated rats, compared with control animals (PTU-treated: 252.16 ± 78.43 pg/mg protein, $n=5$ and controls: 47.49 ± 18.58 pg/mg protein with $n=7$; Fig. 3C).

We also analyzed, by Western blot, the content of the BDNF receptors, TrkB and p75, in the total brain homogenate and in the PSD fractions. As shown in Figure 4A and B, we observed a reduction in TrkB content in the PSD fraction of PTU-treated rats, compared with controls ($68 \pm 2.5\%$ of TrkB content in PTU-treated rats relative to controls $p<0.01$, $n=3$). Conversely, we observed higher levels of TrkB in total telencephalon homogenate from PTU-treated rats, compared with controls ($131 \pm 15\%$ of TrkB content in PTU-treated rats relative to controls $p<0.01$, $n=5$) (Fig. 4A, B). Importantly, the content of p75 receptor in the PSD and total homogenate was similar in control and PTU-treated rats (Fig. 4A, B). Finally, we analyzed the TrkB content by immunohistochemistry in the same brain areas where BDNF was analyzed (Fig. 4C). We

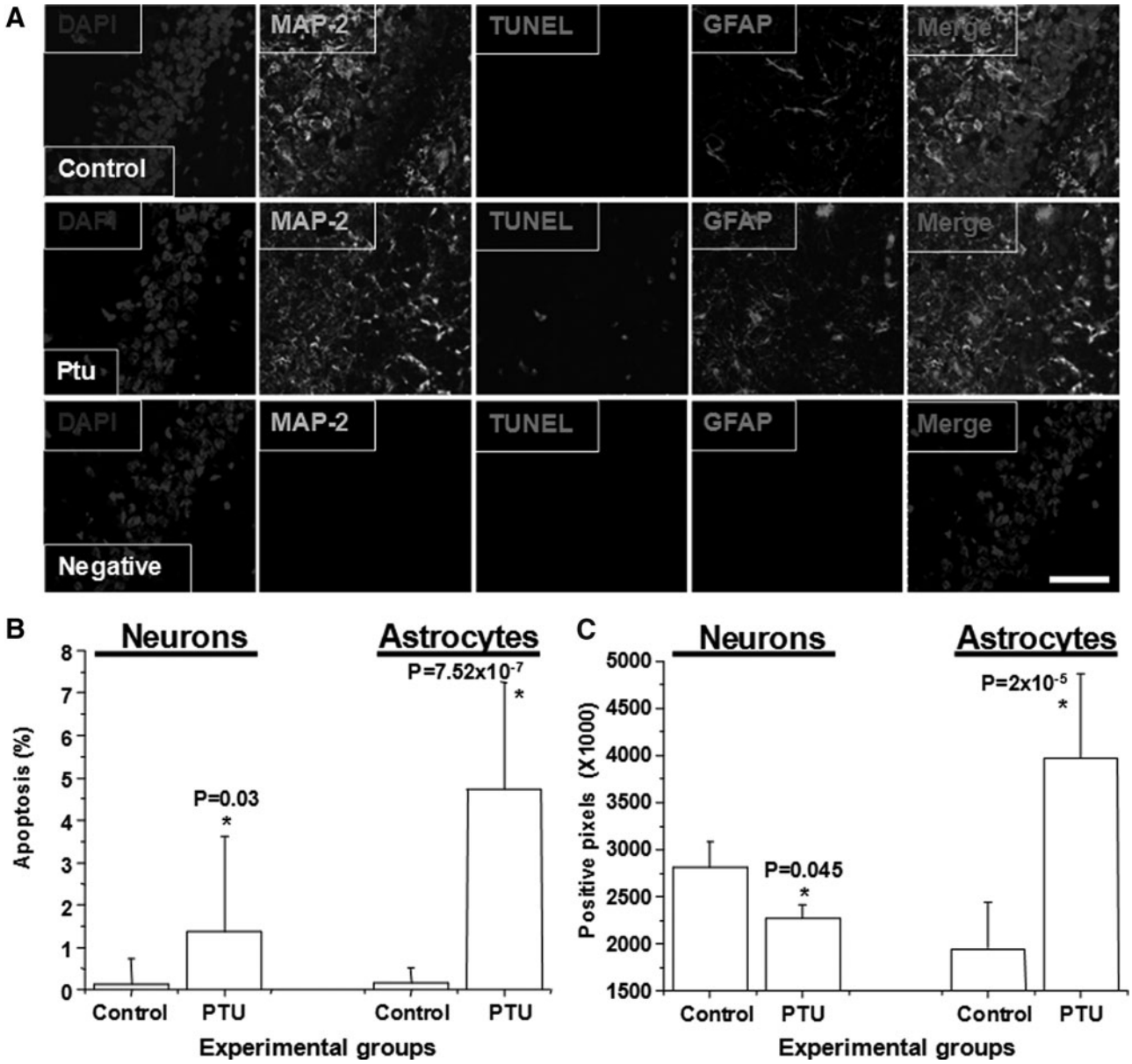

FIG. 2. The hippocampus of hypothyroid adult rat present gliosis and apoptosis. Adult rats were treated or not with 0.05% PTU for 20 days. Then the brain was recovered, fixed as described in "Materials and Methods" and analyzed for the presence of specific proteins by confocal microscopy. **(A)** Gliosis and apoptosis were analyzed at the pyramidal neurons layer of CA3 from tissue sections of the hippocampus of normal rats (control) and hypothyroid rats (PTU treated rats). MAP-2 was used as a neuronal marker (fluorescein isothiocyanate). GFAP was used as a glial marker (CY5). DAPI was used as nuclear marker. In the last row of the figure representative pictures of negative controls for MAP-2 or GFAP antibodies and TUNEL or DAPI are shown. The word negative in this row stands for those brain slices that were incubated with the isotype-matched antibody of MAP-2 or GFAP antibody and for those brain slices that were not stained for TUNEL. The size of the bar is 50 μm. **(B)** Quantification of neuronal and astrocyte apoptosis at the CA3 layer of control and hypothyroid adult rats. 100% of neurons or astrocytes in the field were calculated by counting the total number of cells that stained for MAP-2 or GFAP respectively. The percentage of apoptotic neurons or astrocytes were calculated by counting those cells that stained for MAP-2 or GFAP respectively and co-stained for TUNEL and divided for the total number of the respective type of cell. The analysis was performed using three brain slices per animal and four animals per condition. **(C)** Quantification of neurons and astrocytes at the CA3 of the hippocampus of control and hypothyroid rats (PTU-treated rats). Neurons and astrocytes were quantified by counting the number of cells that were stained by MAP-2 and GFAP respectively. MAP-2 and GFAP detection was performed by using image software, sodium–iodide symporter advance research (NIKON) in the hippocampus field. * indicates significant difference (four animals were analyzed per condition, $p < 0.05$).

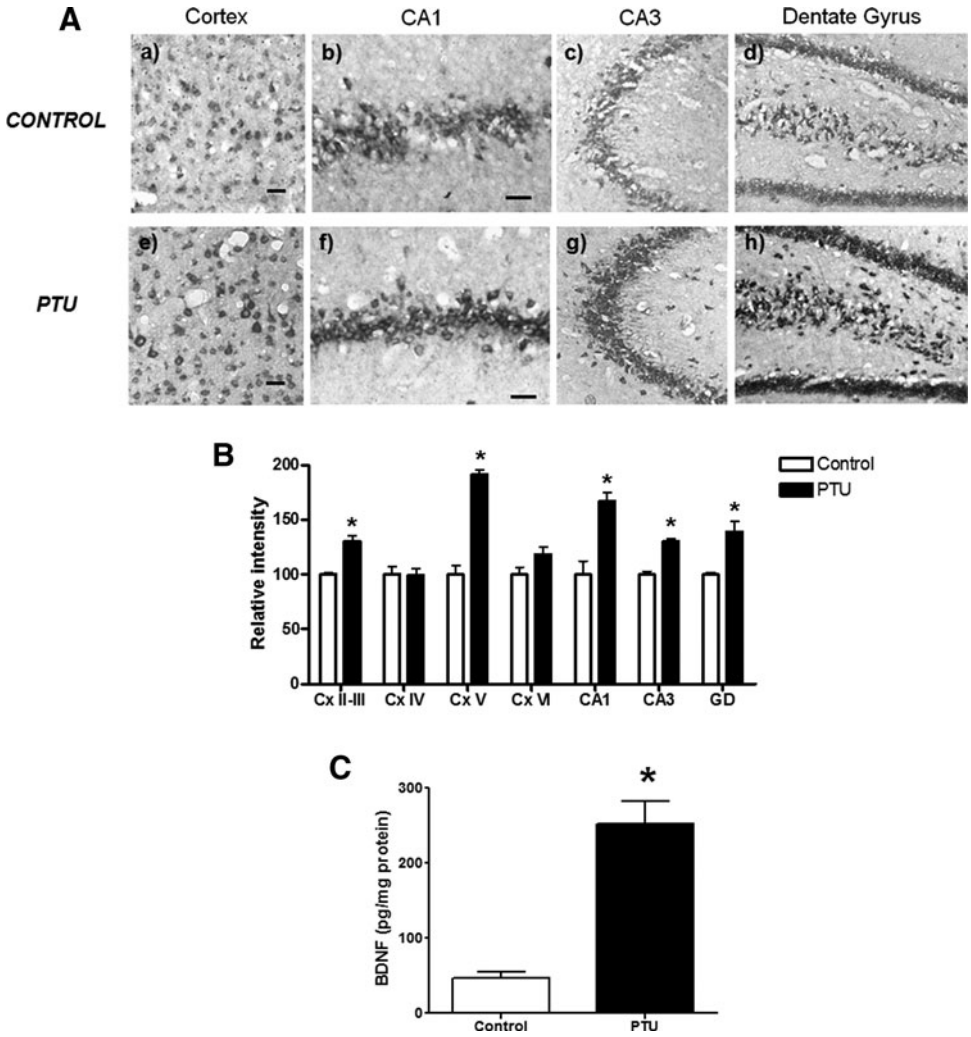

FIG. 3. Increased expression of BDNF exon V in the hippocampus and parietal cortex of hypothyroid adult rats. **(A)** Representative photomicrographs of *in situ* hybridization assay for BDNF mRNA in control rats **(a–d)** and hypothyroid rats (PTU-treated rats) **(e–h)**. The photomicrographs shown are from parietal cortex layer V **(a, e)**, CA1 hippocampal region **(b, f)**, CA3 hippocampal region **(c, g)**, and dentate gyrus **(d, h)** ($n = 3$, the scale bar corresponds to 200 μm for **(a, b, e, f)** to 100 μm for **(c, d, g, h). (B)** Quantification of the relative intensity of BDNF mRNA hybridization assay at the parietal cortex layers II–VI and hippocampal regions of control and hypothyroid rats (PTU-treated rats). **(C)** Quantification of BDNF peptide by enzyme linked immunosorbent assay in the total telencephali of control and hypothyroid rats (PTU treated rats). PTU-treated: 252.16 ± 78.43 pg/mg protein ($n = 5$) and control: 47.49 ± 18.58 pg/mg protein $n = 7$. The statistical analyses were t student comparing control versus PTU-treated rats. * indicates $p < 0.01$. BDNF, brain-derived neurotrophic factor.

observed a reduced stain for this protein in the dendrites of neurons at the layer V of the neocortex, CA1, CA2, CA3, and dentate gyrus.

Hypothyroidism reduces NMDA receptor contents in PSDs

To evaluate the effect of hypothyroidism on the content of NR1 and NR2A/B subunits of the NMDAr in the PSDs of normal and PTU rats, we performed Western blot and immunoprecipitation analysis in brains of control and PTU-treated rats. As observed in Figure 5A and B, a significant reduction in the content of NR2A/B was observed in the PSDs of PTU-treated rats (NR2A/B content in the PSD: $72 \pm 7.63\%$, $p < 0.05$, $n = 3$). In contrast, we observed a slight but significant increase of this subunit in the total fraction of telencephalon homogenates from PTU-treated rats (NR2A/B content in the total homogenate: $126 \pm 13\%$, $p < 0.05$, $n = 5$).

The NR1 subunit was also significantly reduced in the PSDs from PTU-treated rats ($75 \pm 5.5\%$, $p < 0.05$, $n = 5$), but no significant changes were observed in the content of NR1 in the total fraction of telencephalon homogenates (Fig. 5A, B). We also analyzed the association ratio of NR1 and NR2A by co-immunoprecipitation experiments (Fig. 5C, D). NR2A was immunoprecipitated from S2 fraction (see "Materials and Methods"). NR2A and NR1 contents were analyzed from the NR1 immunoprecipitated fraction by Western blot using specific antibodies directed to NR2A and NR1 subunits (Fig. 5C). The values obtained from densitometric analysis of NR1 and NR2A bands were used to determine the association ratio between both proteins (NR1/NR2A). As shown in Figure 5D, our results show that the association ratio of NR1/NR2A was

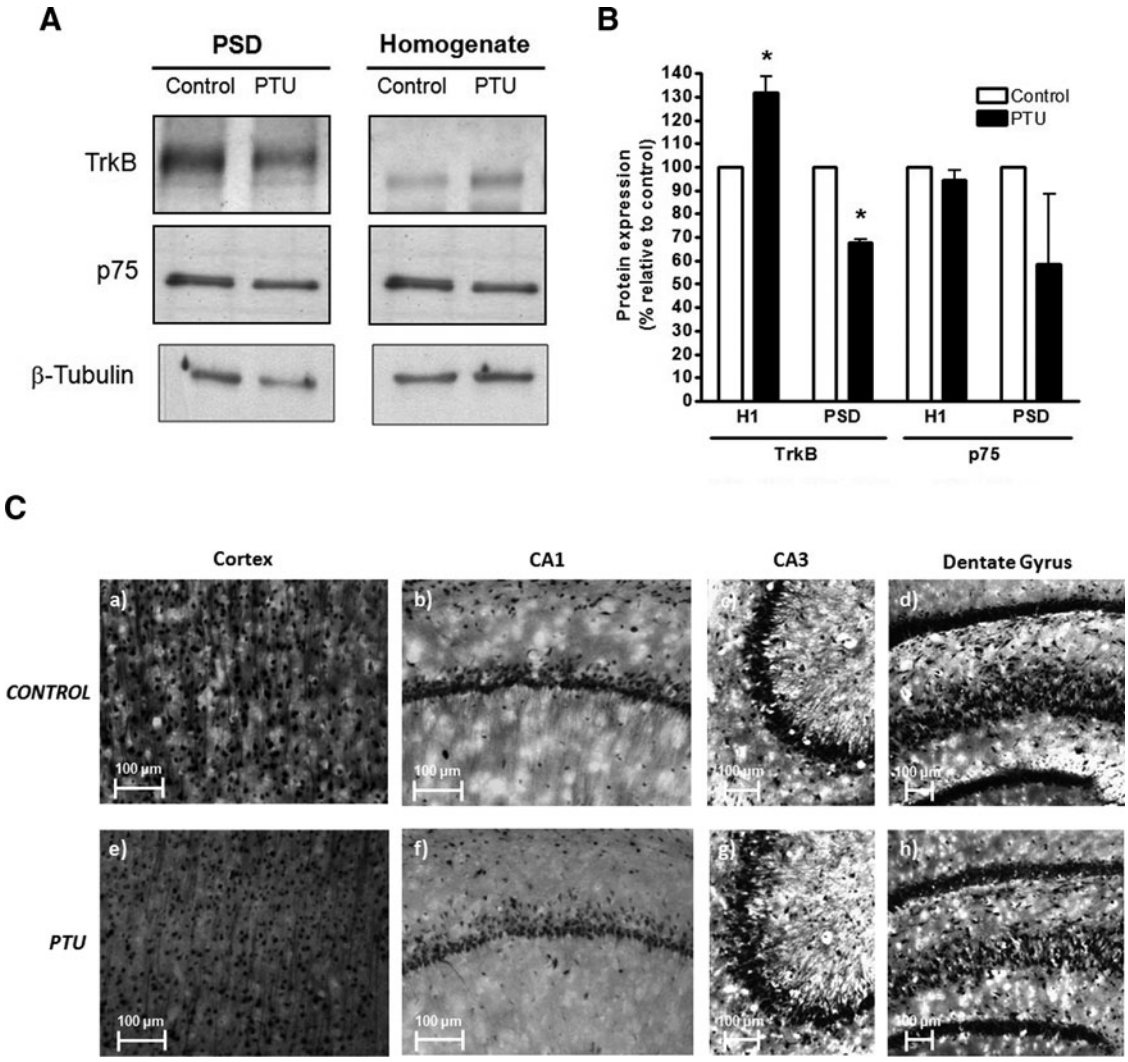

FIG. 4. Reduction of TrkB in the PSD of adult hypothyroid telencephalon. **(A)** Representative pictures of Western blots for TrkB, p75, and β-tubulin from PSD and total telencephalon homogenate from control or PTU-treated rats ($n = 10$). β-tubulin corresponded to the loading control. **(B)** Densitometric analysis to quantify the intensity of the bands for TrkB and p75 from the immunoblots of total telencephalon homogenate (H1) and PSD both control and PTU-treated rats. The band intensity for samples from PTU-treated rats was calculated as the percentage related to its control considered as 100%. TrkB was significantly reduced (*) at PSD and significantly increased at total telencephalon homogenate (*) ($n = 3$, $p < 0.05$). **(C)** Representative pictures of immunohistochemistry for TrkB at the hippocampus of control **(a–d)** and PTU-treated **(e–h)** rats ($n = 3$ per condition). TrkB, tyrosine receptor kinase B; PSD, postsynaptic density.

reduced to 55% in S2 of PTU-treated rats compared with control rats ($p < 0.01$, $n = 5$).

Because a significant reduction in the content of NR1, NR2A/B, and TrkB was observed at the PSD from hypothyroid animals, we analyzed, by transmission electron microscopy, the thickness of PSD in these fractions and also from the glutamatergic synapses of the stratum radiatum of the CA3 (Fig. 6). To assess glutamatergic synapses from the CA3, we studied those synapses located in the proximal region of basal dendrites from CA3 pyramidal neurons. In this region of the stratum radiatum, mossy fibres and commissural synapses are found (Fig. 6A).

Glutamatergic synapses are easily identified by electron microscopy, because they are asymmetrical. Representative pictures of electron micrograph of basal glutamatergic synapses in CA3 region for control and hypothyroid rats are shown in Figure 6B and C, respectively. Representative electron micrographs of PSD fractions are shown from control (Fig. 6D) and hypothyroid rats (Fig. 6E). A quantitative analysis at defined CA3 regions demonstrated a decrease in PSD thickness in CA3 of hypothyroid rats compared with control animals (Fig. 6E). Instead, at the presynaptic regions, the diameter of neurotransmitter vesicle was comparable between hypothyroid and control rats (Fig. 6E).

Discussion

In this study we have shown evidence, at the cellular and molecular level, for the deleterious effects of hypothyroidism in adult brain regions like the hippocampus. Our findings contribute new evidence indicating that adult hypothyroidism is harmful for this organ (29). Our results showed an

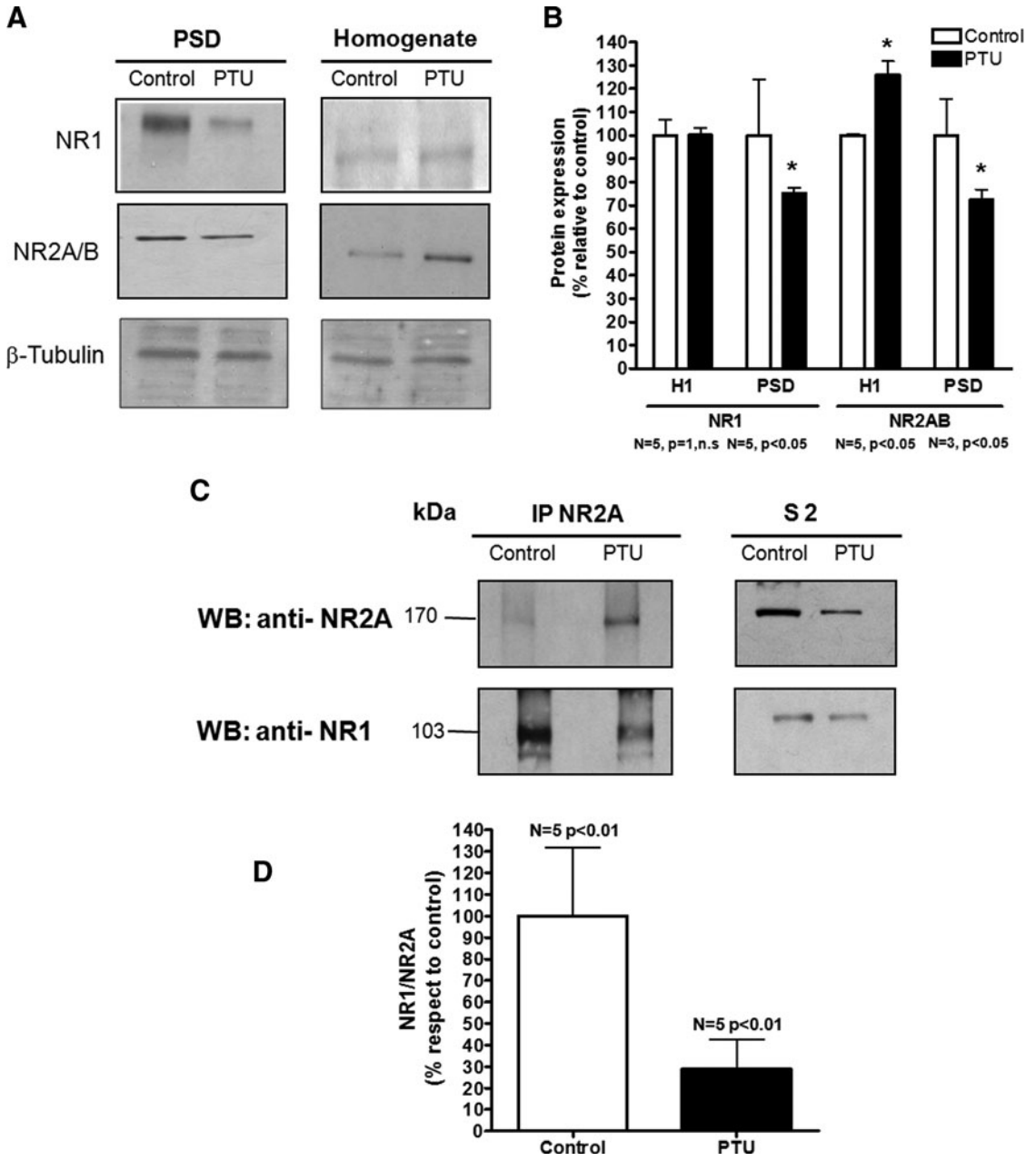

FIG. 5. Reduction in the content of NR1 associated with NR2A in the PSD of hypothyroid adult rats. **(A)** Representative immunoblots for NR1 and NR2A/B detection in PSD and total telencephalon of control and hypothyroid rats (PTU-treated rats). **(B)** Densitometric analyses of the NR1 and NR2A/B bands from the immunoblots of total telencephalon homogenate (H1) and PSD of control and PTU-treated rats. The intensity band for NR1 and NR2A/B of the control rats was considered as 100% and the bands for hypothyroid adult rats were related to those of the control rats. (*) indicates that the content of NR2A/B and NR1 was significantly reduced in the PSD from adult hypothyroid rats ($n=3$). **(C)** Representative photography of immunoblots for NR2A and NR1 that were immunoprecipitated and coimmunoprecipitated respectively from synaptosomes 2 (S2) of control and hypothyroid adult rats. **(D)** Densitometric analysis of NR1 and NR2A bands from the immunoblots of NR2A and NR1 immunoprecipitation and coimmunoprecipitation respectively from S2 of control and PTU-treated rats. The intensity of the band for NR1 and NR2A of control rats was designated as 100%, and the percentages of these bands for hypothyroid adult rats were calculated with respect to the control rats. The PSD from hypothyroid adult rats had a significantly reduced (*) content of NR1 associated to NR2A, compared with control rats ($n=5$). NR1, N-methyl-D-aspartate receptor 1; NR2A/B, N-methyl-D-aspartate receptor 2A/B.

increase in TUNEL reaction in the hypothyroid CA3 hippocampal region, which supports the notion that there is apoptosis process in this area. Consistent with this finding is the report of Alva-Sanchez *et al.* (16), showing an increase in the expression of apoptotic signaling molecules such as Bax/Bcl2 and cell damage in the CA3 hippocampal region during hypothyroidism. Our finding is not only in agreement with this data, but also indicates that apoptosis in the CA3 region of hypothyroid hippocampus occurs in neurons and astrocytes. In fact, apoptosis is not restrictive to the CA3 region because

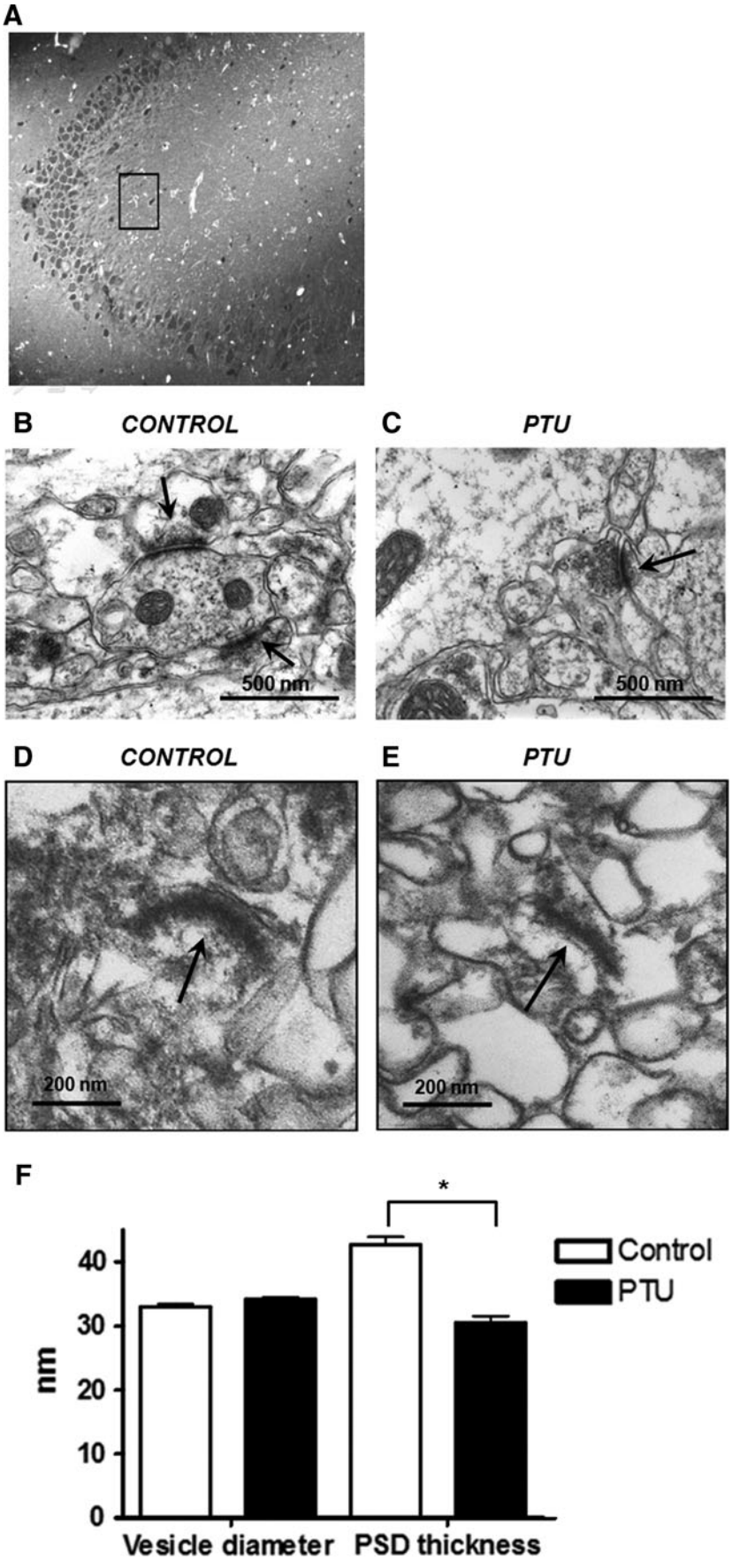

FIG. 6. PSD thickness reduction from the CA3 region of hypothyroid adult rats. **(A)** Semithin section of a CA3 region stained with toluidine blue. The box indicates the region in which micrographs and quantification of PSD and vesicles were performed. Representative transmission electron micrographs of the stratum radiatum at the CA3 region. Arrows indicate the PSD of glutamatergic synapses from CA3 basal dendrites of control **(B)** and hypothyroid (PTU-treated rats) **(C)**. Representative transmission electron micrographs of PSD fractions obtained from the telencephalon of control **(D)** or hypothyroid rats (PTU-treated rats) **(E)**. The arrows indicate the PSD structures; they are in a mixture with, sealed membrane. **(F)** Morphometric analysis of presynaptic vesicle diameter and PSD thickness in hypothyroid (PTU-treated rats) and control rats ($n = 3$ per group, 25–36 synapses analyzed per group). * indicates $p < 0.01$.

we also detected increased levels of apoptosis at CA2 region (data not shown). In agreement with our data, two other studies have shown neuronal apoptosis in other hippocampal regions (*e.g.*, dentate gyrus) (30,31).

We also found that the CA3 region of the hippocampus of hypothyroid rats displays an increase in GFAP staining, suggesting that this region has astrogliosis. This is in agreement with a study performed by Stoica *et al.* (32), who also reported astrogliosis in inherited tertiary hypothyroidism. The presence of both astrogliosis and apoptosis has been described in Alzheimer disease (33), Parkinson disease (34), and HIV infection (35). In all these conditions, it has been suggested that astrogliosis together with apoptosis is a sign of brain inflammation. It will be of interest to evaluate whether astrocytes are secreting chemokines or cytokines that could induce an inflammatory process in the CNS of the hypothyroid rat.

Because BDNF is a neurotrophic factor involved in neuronal protection, cell death, and synaptic plasticity, we also analyzed the brain BDNF content of hypothyroid rats (28). We detected an increase in BDNF in hypothyroid rats. Specifically, BDNF mRNA increased in all hippocampus regions and at the layers II, III, and V of the neocortex. On the other hand, the quantities of BDNF mRNA in the IV and VI neocortex layers were similar in hypothyroid and control rats. These results are not in agreement with reports that BDNF mRNA levels are similar in all brain regions of hypothyroid animals (15). We believe that these differences are due to differences in the probes used to detect BDNF mRNA. Notably, it has been shown that there are eight possible transcripts for BDNF (36) and in the *in situ* hybridization analysis performed in this study we used a cRNA antisense probe specific for the coding exon V; this detects all possible BDNF transcripts. We also analyzed BDNF peptide expression, because this peptide is regulated at the transcriptional level and it is also highly regulated at the transduction and post-secretion level (37). We found that BDNF peptide increased fivefold in the telencephalon of hypothyroid rats. This is consistent with the mRNA results. These results suggest that, in the hypothyroid state, there is an increase in BDNF production, probably as a response to a cellular stress.

The content of BDNF peptide was analyzed by ELISA; this assay does not discriminate between BDNF and its precursor ProBDNF. This is an important point because both molecules are co-secreted but ProBDNF has biological activity per se that could be different to that of BDNF (38). Regarding this, it has been proposed that ProBDNF has an action opposite to that of BDNF and that its action is mediated by p75 receptor (39). Instead, BDNF preferentially interacts with TrkB (37). In the present study, we found that the content of p75 was similar in hypothyroid and control rats, but the content of TrkB in PSDs was decreased in the telencephalon of hypothyroid rats. Consistent with this result is the observation of reduced stain for TrkB at the dendrites and soma of pyramidal neurons in the hippocampal regions of hypothyroid rats. Given that our results have shown that BDNF increases in the hippocampal regions of hypothyroid rats and TrkB decreases, it is possible that TrkB could be downregulated at synaptic contacts in the hippocampus of these rats. In fact, TrkB was decreased in PSDs but its content was higher in the whole telencephalon of hypothyroid rats compared with controls. Downregulation of TrkB, due to high levels of BDNF, has been reported (40). Thus, the observation of reduced amounts of TrkB, in the PSDs that contain normal amounts of p75 suggests that, in the hippocampus of hypothyroid rats, the action BDNF is mediated mainly by p75 and not by TrkB. This is relevant since the capacity to play opposite roles in neuronal survival and synapse potentiation, depending on the type of receptor that is preferentially expressed at the surface of the target cell (TrkB or p75), has been attributed to BDNF (28,41). It has also been reported that the interaction of BDNF or ProBDNF with p75 has deleterious effects on glutamatergic neurons, for example apoptosis induction and damaging of glutamatergic synapses (41). With respect to glutamatergic synapses, we found a reduction in the content of NR1 and NR2A/B NMDA subunits in the PSD fractions and in the number of NR1 subunits associated with the NR2A subunit, suggesting that PSDs in the hypothyroid state contained reduced amounts of NMDA receptors. A reduction in the number of NMDA receptors at the postsynaptic neuron has been associated with impaired glutamatergic synaptic function (42). Even though, the sizes of the vesicles were similar in hypothyroid and control glutamatergic synapses (Fig. 6D), PSDs were significantly thinner in hypothyroid rats than control rats. The reduction in the PSD thickness correlated with the drop in the content of NR1, NR2A/B, and TrkB in the PSD fraction, supporting the concept that glutamatergic synapses in this region could be impaired.

In summary, in this study we found apoptosis, gliosis, and alterations in PSDs in the hippocampus of hypothyroid rats, supporting the notion that hypothyroidism is harmful to this brain region.

Acknowledgments

The authors are supported by grants FONDECYT no. 1100926, FONDECYT no. 1070352, FONDECYT no. 1085281, FONDECYT no. 1100926, FONDECYT no. 3070018, FONDECYT no. 3100090, FONDECYT no. 11075060, and FONDECYT no. 1100926, Millennium Institute on Immunology and Immunotherapy (P-09-016-F), Millennium Nucleus (P07-011-F) and Proyecto Interno Universidad Andrés Bello DI-01-44-08.

Disclosure Statement

No competing financial interests exist.

References

1. Bauer M, Heinz A, Whybrow PC 2002 Thyroid hormones, serotonin and mood: of synergy and significance in the adult brain. Mol Psychiatry **7:**140–156.
2. Bernal J, Nunez J 1995 Thyroid hormones and brain development. Eur J Endocrinol **133:**390–398.
3. Farwell AP, Dubord-Tomasetti SA, Pietrzykowski AZ, Leonard JL 2006 Dynamic nongenomic actions of thyroid hormone in the developing rat brain. Endocrinology **147:** 2567–2574.
4. Gomes FC, Maia CG, de Menezes JR, Neto VM 1999 Cerebellar astrocytes treated by thyroid hormone modulate neuronal proliferation. Glia **25:**247–255.
5. Bernal J 2007 Thyroid hormone receptors in brain development and function. Nat Clin Pract Endocrinol Metab **3:**249–259.
6. Silva JE 2003 The thermogenic effect of thyroid hormone and its clinical implications. Ann Intern Med **139:**205–213.

7. Bauer M, London ED, Silverman DH, Rasgon N, Kirchheiner J, Whybrow PC 2003 Thyroid, brain and mood modulation in affective disorder: insights from molecular research and functional brain imaging. Pharmacopsychiatry **36 Suppl 3:**S215–221.
8. Lass P, Slawek J, Derejko M, Rubello D 2008 Neurological and psychiatric disorders in thyroid dysfunctions. The role of nuclear medicine: SPECT and PET imaging. Minerva Endocrinol **33:**75–84.
9. Correia N, Mullally S, Cooke G, Tun TK, Phelan N, Feeney J, Fitzgibbon M, Boran G, O'Mara S, Gibney J 2009 Evidence for a specific defect in hippocampal memory in overt and subclinical hypothyroidism. J Clin Endocrinol Metab **94:** 3789–3797.
10. Rovet JF, Ehrlich R 2000 Psychoeducational outcome in children with early-treated congenital hypothyroidism. Pediatrics **105:**515–522.
11. Wekking EM, Appelhof BC, Fliers E, Schene AH, Huyser J, Tijssen JG, Wiersinga WM 2005 Cognitive functioning and well-being in euthyroid patients on thyroxine replacement therapy for primary hypothyroidism. Eur J Endocrinol **153:**747–753.
12. Alzoubi KH, Gerges NZ, Aleisa AM, Alkadhi KA 2009 Levothyroxin restores hypothyroidism-induced impairment of hippocampus-dependent learning and memory: behavioral, electrophysiological, and molecular studies. Hippocampus **19:**66–78.
13. Alzoubi KH, Gerges NZ, Alkadhi KA 2005 Levothyroxin restores hypothyroidism-induced impairment of LTP of hippocampal CA1: electrophysiological and molecular studies. Exp Neurol **195:**330–341.
14. Lee PR, Brady D, Koenig JI 2003 Thyroid hormone regulation of N-methyl-D-aspartic acid receptor subunit mRNA expression in adult brain. J Neuroendocrinol **15:**87–92.
15. Alvarez-Dolado M, Iglesias T, Rodriguez-Pena A, Bernal J, Munoz A 1994 Expression of neurotrophins and the trk family of neurotrophin receptors in normal and hypothyroid rat brain. Brain Res Mol Brain Res **27:**249–257.
16. Alva-Sanchez C, Sanchez-Huerta K, Arroyo-Helguera O, Anguiano B, Aceves C, Pacheco-Rosado J 2009 The maintenance of hippocampal pyramidal neuron populations is dependent on the modulation of specific cell cycle regulators by thyroid hormones. Brain Res **1271:**27–35.
17. Legrand J 1967 Analysis of the morphogenetic action of thyroid hormones on the cerebellum of young rats. Arch Anat Microsc Morphol Exp **56:**205–244.
18. Osorio M, Wohllk N, Pineda G 1993 Treatment of hyperthyroidism during pregnancy: experience with 19 cases. Rev Med Chil **121:**660–665.
19. Madeira MD, Cadete-Leite A, Andrade JP, Paula-Barbosa MM 1991 Effects of hypothyroidism upon the granular layer of the dentate gyrus in male and female adult rats: a morphometric study. J Comp Neurol **314:**171–186.
20. Eugenin EA, D'Aversa TG, Lopez L, Calderon TM, Berman JW 2003 MCP-1 (CCL2) protects human neurons and astrocytes from NMDA or HIV-tat-induced apoptosis. J Neurochem **85:**1299–1311.
21. Eugenin J, Nicholls JG, Cohen LB, Muller KJ 2006 Optical recording from respiratory pattern generator of fetal mouse brainstem reveals a distributed network. Neuroscience **137:**1221–1227.
22. Aliaga E, Rage F, Tapia-Arancibia L, Bustos G 1999 Negative regulation of brain-derived neurotrophic factor mRNA expression by kainic acid in substantia nigra. Brain Res Mol Brain Res **71:**341–344.
23. Aliaga E, Arancibia S, Givalois L, Tapia-Arancibia L 2002 Osmotic stress increases brain-derived neurotrophic factor messenger RNA expression in the hypothalamic supraoptic nucleus with differential regulation of its transcripts. Relation to arginine-vasopressin content. Neuroscience **112:**841–850.
24. Kokaia Z, Bengzon J, Metsis M, Kokaia M, Persson H, Lindvall O 1993 Coexpression of neurotrophins and their receptors in neurons of the central nervous system. Proc Natl Acad Sci USA **90:**6711–6715.
25. Szapacs ME, Mathews TA, Tessarollo L, Ernest Lyons W, Mamounas LA, Andrews AM 2004 Exploring the relationship between serotonin and brain-derived neurotrophic factor: analysis of BDNF protein and extraneuronal 5-HT in mice with reduced serotonin transporter or BDNF expression. J Neurosci Methods **140:**81–92.
26. Smith PK, Krohn RI, Hermanson GT, Mallia AK, Gartner FH, Provenzano MD, Fujimoto EK, Goeke NM, Olson BJ, Klenk DC 1985 Measurement of protein using bicinchoninic acid. Anal Biochem **150:**76–85.
27. Blahos J 2nd, Wenthold RJ 1996 Relationship between N-methyl-D-aspartate receptor NR1 splice variants and NR2 subunits. J Biol Chem **271:**15669–15674.
28. Chao MV 2003 Neurotrophins and their receptors: a convergence point for many signalling pathways. Nat Rev Neurosci **4:**299–309.
29. Koromilas C, Liapi C, Schulpis KH, Kalafatakis K, Zarros A, Tsakiris S 2010 Structural and functional alterations in the hippocampus due to hypothyroidism. Metab Brain Dis **25:**339–354.
30. Ambrogini P, Cuppini R, Ferri P, Mancini C, Ciaroni S, Voci A, Gerdoni E, Gallo G 2005 Thyroid hormones affect neurogenesis in the dentate gyrus of adult rat. Neuroendocrinology **81:**244–253.
31. Desouza LA, Ladiwala U, Daniel SM, Agashe S, Vaidya RA, Vaidya VA 2005 Thyroid hormone regulates hippocampal neurogenesis in the adult rat brain. Mol Cell Neurosci **29:**414–426.
32. Stoica G, Lungu G, Xie X, Abbott LC, Stoica HM, Jaques JT 2007 Inherited tertiary hypothyroidism in Sprague-Dawley rats. Brain Res **1148:**205–216.
33. Li C, Zhao R, Gao K, Wei Z, Yin MY, Lau LT, Chui D, Hoi Yu AC 2011 Astrocytes: implications for neuroinflammatory pathogenesis of Alzheimer's disease. Curr Alzheimer Res **8:**67–80.
34. Hirsch EC, Breidert T, Rousselet E, Hunot S, Hartmann A, Michel PP 2003 The role of glial reaction and inflammation in Parkinson's disease. Ann NY Acad Sci **991:**214–228.
35. Sabri F, Titanji K, De Milito A, Chiodi F 2003 Astrocyte activation and apoptosis: their roles in the neuropathology of HIV infection. Brain Pathol **13:**84–94.
36. Timmusk T, Palm K, Metsis M, Reintam T, Paalme V, Saarma M, Persson H 1993 Multiple promoters direct tissue-specific expression of the rat BDNF gene. Neuron **10:**475–489.
37. Greenberg ME, Xu B, Lu B, Hempstead BL 2009 New insights in the biology of BDNF synthesis and release: implications in CNS function. J Neurosci **29:**12764–12767.
38. Woo NH, Teng HK, Siao CJ, Chiaruttini C, Pang PT, Milner TA, Hempstead BL, Lu B 2005 Activation of p75NTR by proBDNF facilitates hippocampal long-term depression. Nat Neurosci **8:**1069–1077.
39. Teng HK, Teng KK, Lee R, Wright S, Tevar S, Almeida RD, Kermani P, Torkin R, Chen ZY, Lee FS, Kraemer RT, Nykjaer A, Hempstead BL 2005 ProBDNF induces neuronal apoptosis via activation of a receptor complex of p75NTR and sortilin. J Neurosci **25:**5455–5463.

40. Unsain N, Montroull LE, Masco DH 2009 Brain-derived neurotrophic factor facilitates TrkB down-regulation and neuronal injury after status epilepticus in the rat hippocampus. J Neurochem **111:**428–440.
41. Dechant G, Barde YA 2002 The neurotrophin receptor p75(NTR): novel functions and implications for diseases of the nervous system. Nat Neurosci **5:**1131–1136.
42. Perez-Otano I, Ehlers MD 2004 Learning from NMDA receptor trafficking: clues to the development and maturation of glutamatergic synapses. Neurosignals **13:**175–189.

Address correspondence to:
Claudia Riedel, Ph.D.
Laboratorio de Biología Celular y Farmacología
Departamento de Ciencias Biológicas
Universidad Andrés Bello
República 217
Santiago 830000
Chile

E-mail: riedel@unab.cl